A1013

Lattice-Boltzmann simulation of two-phase flows in the GDL and MPL of Polymer Electrolyte Fuel Cells

Patrick Sarkezi-Selsky (1), Maren Rastedt (2), Arnulf Latz (1,3), Thomas Jahnke (1)
(1) German Aerospace Center (DLR), Institute of Engineering Thermodynamics
Pfaffenwaldring 38-40, 70569 Stuttgart, Germany
(2) German Aerospace Center (DLR), Institute of Networked Energy Systems
Carl-von-Ossietzky-Str. 15, 26129 Oldenburg, Germany
(3) Helmholtz Institute Ulm for Electrochemical Energy Storage (HIU)
Albert-Einstein-Allee 11, 89081 Ulm, Germany
Tel.: +49 711 6862-498
Fax: +49 711 6862-747
Patrick.Sarkezi-Selsky@dlr.de

Abstract

Polymer Electrolyte Fuel Cells (PEMFCs) are increasingly approaching the focus of research as a promising alternative to commercial battery electrical cars. Reliable supply of energy up to high loads, good efficiency and refueling within minutes makes fuel cells compelling for drive technologies, in particular for high load applications, e.g., public transport or commercial vehicles. To meet the requirements for load cycling and performance of such applications, a simultaneous transport of educts and products through the porous layers of the cell has to be maintained to prevent unwanted scenarios like flooding [1]. This is a demanding task and the underlying multiphase processes are very complex and yet scarcely understood, but experiments in this field are costly and not always accessible. On this account simulations are needed to model those transport processes and to foster a better understanding of multiphase flows in the porous electrodes.
In our work we simulate two-phase flows within gas diffusion layers (GDLs) using a 3D Lattice-Boltzmann model based on the color-gradient model (CGM) by Rothman and Keller [2]. Simulations are carried out on microstructural geometries obtained from binarized µCT-scans for a gas diffusion medium based on a Freudenberg GDL with hydrophobic treatment and MPL. We include the MPL as a boundary layer, assuming that liquid phase flow into the GDL occurs primarily via the macropores of the MPL. Applying different capillary pressures, we derive wetting phase saturations and subsequently capillary pressure-saturation curves. This work covers furthermore a study on the impact of different contents of hydrophobic binder (PTFE) on the transport of liquid water inside the porous media.
The results of the simulation model meet our expectations and acknowledge the impeding effect of PTFE on water transport through the GDL. Increasing the load of hydrophobic binder leads to lower saturations for a given capillary pressure, indicating a reduced flooding tendency.

Introduction

Degradation phenomena are still one of the main bottlenecks for a widespread market entry of PEMFCs in the automotive sector [3]. Many degradation mechanisms are already identified by now, but not quantified yet. Others are only suspected to happen, but further investigations by experiments are still missing. In particular, the degradation of the GDL and its impact on performance degradation is not yet well understood. Hydrophobic binder as an additive impregnated on the porous gas diffusion layers has been established as state-of-the-art over the last decade, since its impact on cell performance by improving water management and impeding flooding is well known [4]. Ex-situ experiments showed furthermore, that PTFE degrades at elevated flow rates, or under oxidative conditions such as in hot hydrogen peroxide baths [5, 6]. But the studies were mainly limited to qualitative analyses of the PTFE loss. Quantitative analysis of binder degradation is, to the author's best knowledge, up to now still missing. Simulations cannot replace these important investigations, but they can help to understand the effects of degradation on effective transport parameters by drawing a connection between PTFE content and e.g. a relation between capillary pressure and saturation or permeability. These results would in the end also be useful for cell-level degradation models.

1. Scientific Approach

The aim of this work is to simulate multiphase transport within the porous gas diffusion layers (GDLs) and microporous layers (MPL) of low temperature PEMFCs using microstructural information from µCT images. The intention of this effort is to derive effective transport parameters as a function of the hydrophobic binder (PTFE) content. Dependencies such as capillary pressure-saturation relationships will then help to deepen understanding and to quantify the impact of PTFE on the liquid water transport in PEMFCs.

2. Simulation Model

Multiphase transport within the porous GDL structures is simulated using the Lattice-Boltzmann method (LBM), which is a mesoscopic modelling approach based on solving the Boltzmann equation discretized on a lattice with m dimensions and n velocity sets (DmQn model).

$$f_i(\mathbf{x} + \mathbf{e}_i\Delta t, t + \Delta t) = f_i(\mathbf{x}, t) + \Omega\big(f_i(\mathbf{x}, t)\big) \tag{1}$$

The fundamental quantity $f_i(\mathbf{x}, t)$ denotes a velocity distribution as function of a state vector $\mathbf{x}$ in 2*m-dimensional phase space, with i indicating a specific lattice direction $\mathbf{e}_i$. A generalized operator $\Omega\big(f(\mathbf{x}, t)\big)$ is acting as a source term and, in the case of single-phase modeling, equals a single-phase collision operator. In this work the formulation by Bhatnagar, Gross and Krook [7] (eq. (2)) was chosen as follows:

$$\Omega^{\mathrm{BGK}}\big(f_i(\mathbf{x}, t)\big) = \omega_{eff}[f_i(\mathbf{x}, t) - f_i^{eq}(\mathbf{x}, t)] \tag{2}$$

$$f_i^{\mathrm{single-phase}}(\mathbf{x} + \mathbf{e}_i\Delta t, t + \Delta t) = f_i(\mathbf{x}, t) + \omega_{eff}[f_i(\mathbf{x}, t) - f_i^{eq}(\mathbf{x}, t)] \tag{3}$$

ω_{eff} is a relaxation parameter controlling the speed of approaching the local equilibrium distribution ${f_i}^{eq}$, it can be derived from kinetic theory [8]

$$ {f_i}^{eq}(\mathbf{x},t) = \rho\left(\phi_i + W_i\left[3\mathbf{c}_i \bullet \mathbf{u} + \frac{9}{2}(\mathbf{c}_i \bullet \mathbf{u})^2 - \frac{3}{2}\mathbf{u} \bullet \mathbf{u}\right]\right) \tag{4} $$

where ϕ_i is the fluid's compressibility and W_i and $\mathbf{c}_i$ are lattice-specific weights and velocity sets respectively, $\mathbf{u}$ is the fluid's velocity.
Modelling of multiple phases requires an extension of the numerical scheme to account for interphase interactions. Following the ansatz by Rothman & Keller [2] we adopted the color-gradient model (CGM), where two phases are modeled as a 'red' and a 'blue' fluid.

$$ f_i(\mathbf{x},t) = {f_i}^r(\mathbf{x},t) + {f_i}^b(\mathbf{x},t) \tag{5} $$

In this model the surface tension between the two phases is generated by a perturbation operator [9],

$$ {f_i}^{\text{pert}} = {f_i}^{\text{single-phase}} + \Delta {f_i}^{\text{pert}} \tag{6} $$

$$ \Delta {f_i}^{\text{pert}} = A|\mathbf{\Phi}|\left[W_i \frac{(\mathbf{\Phi} \bullet \mathbf{c}_i)^2}{|\mathbf{\Phi}|} - B_i\right] \tag{7} $$

for which a color-gradient $\mathbf{\Phi}$ is defined, approximating the normal to the fluid-fluid interface. This color-gradient is usually calculated by isotropic discretization schemes [10] up to fourth order of accuracy, such as in this work.

$$ \mathbf{\Phi} = \nabla\left(\frac{\rho_r - \rho_b}{\rho_r + \rho_b}\right) \tag{8} $$

Furthermore B_i is depending on the given lattice velocity set $\mathbf{c}_i$ and A is a function of the desired surface tension and the relaxation parameter: [9, 11]

$$ A = \frac{9}{4}\omega_{eff}\sigma \tag{9} $$

Eventually a recoloring operator [12] has to be employed as well to guarantee immiscibility between the two phases.

$$ {f_i}^{r,\ \text{recol}} = \frac{\rho_r}{\rho}{f_i}^{\text{pert}} + \beta\frac{\rho_r\rho_b}{\rho^2}\cos\ (\nu_i)\,{f_i}^{eq}(\mathbf{x}_{\mathbf{u}=\mathbf{0}},t) \tag{10} $$

$$ {f_i}^{b,\ \text{recol}} = \frac{\rho_b}{\rho}{f_i}^{\text{pert}} - \beta\frac{\rho_r\rho_b}{\rho^2}\cos\ (\nu_i)\,{f_i}^{eq}(\mathbf{x}_{\mathbf{u}=\mathbf{0}},t) \tag{11} $$

In the above two equations (10) and (11) β effects the interface thickness and ν_i denotes the angle between the lattice direction $\mathbf{c}_i$ and the color-gradient $\mathbf{\Phi}$. The equilibrium distribution ${f_i}^{eq}(\mathbf{x}_{\mathbf{u}=\mathbf{0}},t)$ is the same as in eq. (4) but with a zero velocity ($\mathbf{u} = \mathbf{0}$).
As a last step, the new distribution functions have to be streamed out for each phase k, by reassigning them along the lattice:

$$ {f_i}^k(\mathbf{x} + \mathbf{e}_i\Delta t, t + \Delta t) = {f_i}^{k,\ \text{recol}}(\mathbf{x},t) \tag{12} $$

3. Boundary conditions

Solid boundaries are modeled by a no-slip condition using the full-way bounce back scheme [13]. Contact angles between fluid-solid and fluid-fluid interfaces are imposed by setting fictitious densities at the solid boundaries using the standard wetting boundary approach [14].

Single phase pressures and therefore also the total system pressure are controlled at in- and outlet boundaries with the formulation of Zou & He [15]. For all other domain boundaries standard periodic boundary conditions are set.

4. Image post-processing

GDL/MPL microstructures were analyzed using the µCT scanning technique for a base area with 2304x2304 µm. The images had a resolution of 0.96 µm per pixel, therefore analysis of the MPL structure was restricted to its macropores (Figure 1). Sampled data was then further filtered in Geodict using a sharpening and a median filter, each with a radius of one voxel.

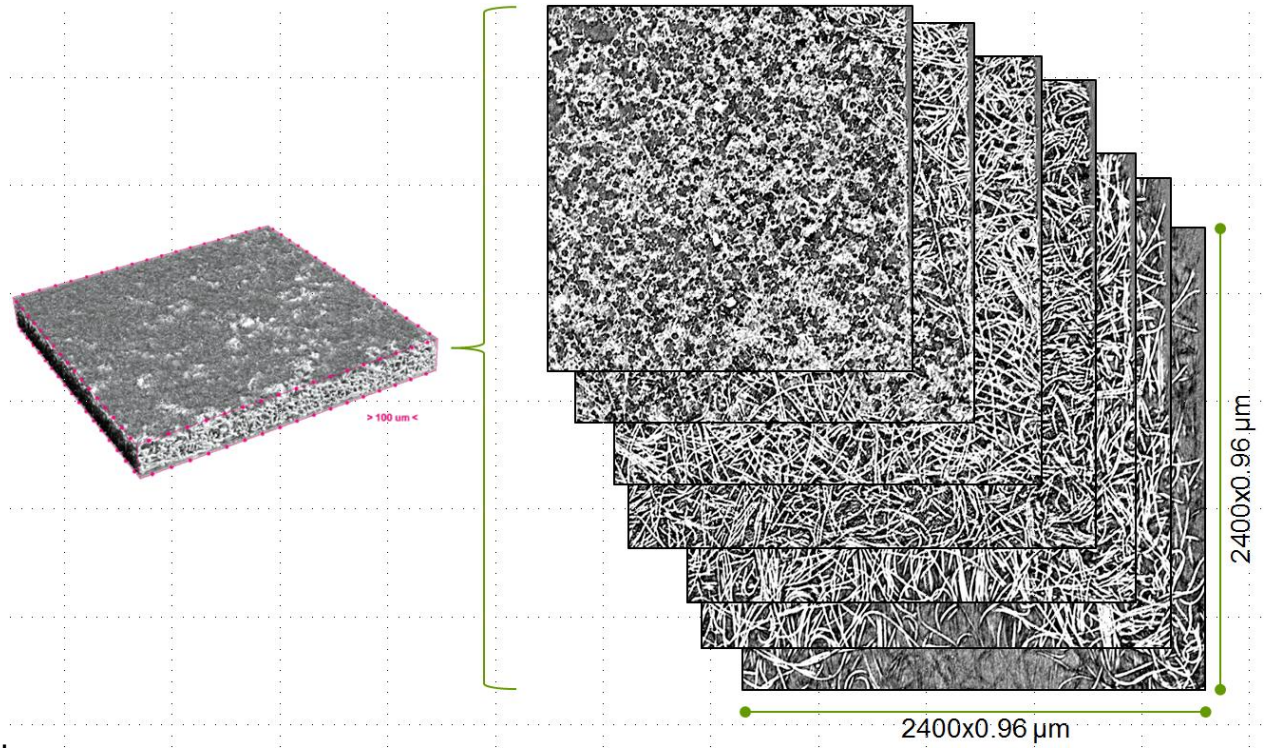

.

Figure 1: µCT-scans from a Freudenberg GDL with hydrophobic treatment and MPL. 3D structural data (left) is obtained by stacking a multitude of 2D images (right).

As a next step, the GDL microstructures were binarized by manual thresholding, for this the surveyed structure was reduced to solely the GDL layers. A sensitivity study on the GDL porosity was conducted to determine an appropriate choice for the gray threshold value as shown in (Figure 2, left). To assure the findings of this analysis, we also simulated pore size distributions (PSDs) within Geodict using different threshold values and compared them to an in-house porosimetry measurement (Figure 3). Based on the

outcome of both studies we chose a gray threshold value of 252 and derived a porosity profile for both, GDL and MPL (Figure 2, right).

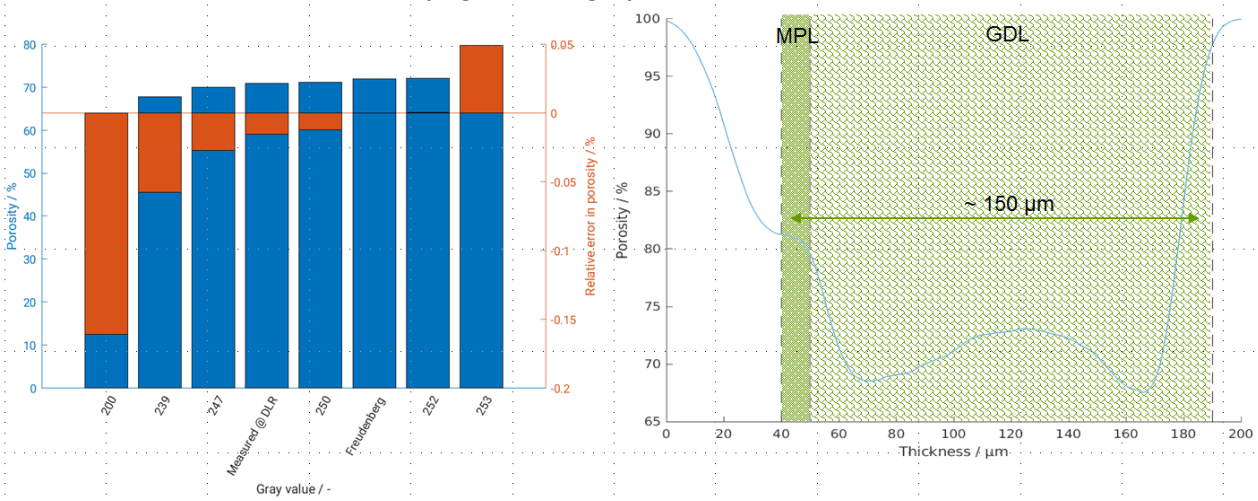

Figure 2: Left: Sensitivity study of porosity as function of the gray threshold for binarization. Right: Porosity profile along GDL/MPL thickness for a gray threshold value of 252.

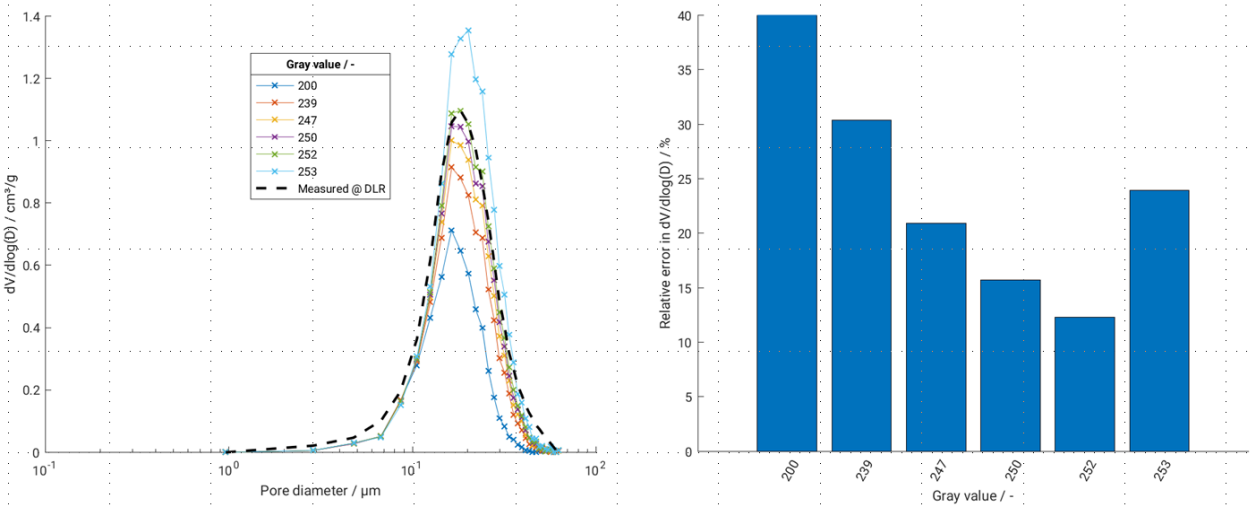

Figure 3: Left: PSDs from simulations in Geodict for different gray threshold values compared to a porosimetry measurement. Right: Relative errors of simulated to measured PSDs.

In a final stage of data post-processing the domain size-dependence of structural properties, i.e., PSDs were analyzed (Figure 4). Finding a compromise between accuracy and time consumption we arrived at a domain size for the GDL structure of 200x200x110 voxel to be used in our LBM simulations. For the MPL data we proceeded in the same way, but cut out only one layer with 200x200x1 voxel from the midst of the MPL thickness to use it as an inlet boundary layer in simulations (see 5. Numerical setup).

Inability to distinguish binder and support material properly is a common problem for CT scanning techniques and it was not solved within the framework of this study. To be able to simulate microstructures with varying amounts of PTFE, we employed Geodict to add binder material artificially within the binarized microstructure. It is self-evident, that this is a source of inaccuracy and this topic might be covered in some future work.

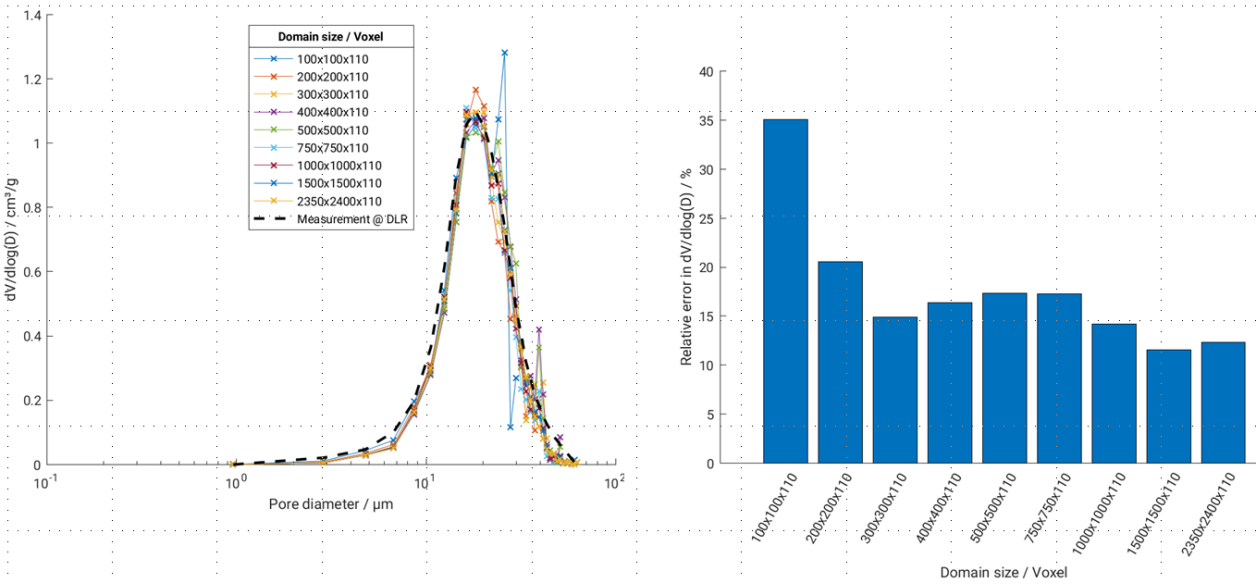

Figure 4: Left: PSDs from simulations in Geodict for different domain sizes compared to a porosimetry measurement. Right: Relative errors of simulated to measured PSDs

5. Numerical setup

In this work the D3Q19 model was used on a simulation domain consisting of the GDL structure (200x200x110 voxels) plus two boundary layers. One of those boundaries was added as a gas phase layer to the top of the GDL geometry (channel side). The other one, the MPL layer, complemented the bottom (MPL side). Assuming that liquid water enters the GDL predominantly through major MPL pores, a variable liquid phase pressure (see section 3) was then imposed on the pore space of the MPL layer. Simultaneously the gas phase pressure was held constant by keeping the gas density on the gas channel side at unity. With this setup a capillary boundary pressure $\Delta p^{cap} = p^{liq} - p^{gas}$ was defined for each simulation (Figure 5).

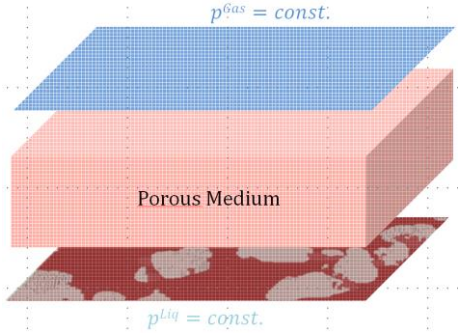

Figure 5: Simulation setup with binarized microstructure (rose) in the middle and gas phase pressure boundary condition (blue) on top (channel side). On the bottom nanopores of the MPL are considered as solid (red), whereas white spots stand for liquid phase inlet through MPL macropores.

Eventually a few simulation parameters inherent to the Lattice-Boltzmann methodology have to be set as well, which were in this work chosen as follows: The kinetic viscosities were set to $\nu^{liq} = \nu^{gas} = 1/5$ and the surface tension to $\sigma = 0.1$. The interface thickness

was adjusted with $\beta = 0.85$. Based on a wide range of literature data the contact angle for the hydrophobic binder was chosen to ${\theta_c}^{PTFE} = 115°$ [16]. For the carbon support the measured value for a single carbon fiber was adapted with ${\theta_c}^{Carbon} = 80°$ [17].

6. Results and discussion

Simulations were carried out for three different contents of PTFE (0, 2.5 and 5 wt%) applying different capillary pressures. These loadings are considerably lower than in common gas diffusion layers, where the binder content is usually between 10 and 20 wt%. This was done intentionally, in order to investigate the effect of PTFE loss as GDL degradation mechanism on the water transport.
For each PTFE content one single simulation was started and equilibrated with a capillary pressure of zero. The endpoint of this simulation was then taken as starting point for further simulations, each with a different capillary pressure, which was in every case preset by varying the liquid phase inlet pressure and keeping the gas boundary pressure at unity (see 5. Numerical setup).
From the equilibrated saturations capillary pressure-saturation curves were derived for all three contents of PTFE, as shown in Figure 6. As it is clearly seen, already small amounts of PTFE have a noticeable effect on the water transport within the microporous structure of the gas diffusion layer. For increasing contents of binder the p_c-S curves show lower saturations for the same capillary pressures. This indicates the hindering effect of PTFE on the water transport as it was presumed. For clearer trends more data points, especially in the area of intermediate saturations, are required and would be helpful for a more detailed comparison. But the simulations are time consuming and results still pending. Equally interesting would be the analysis of permeabilities and their dependence on not just saturation and capillary pressure, but also on the content of PTFE. This is planned to be covered in a future work.

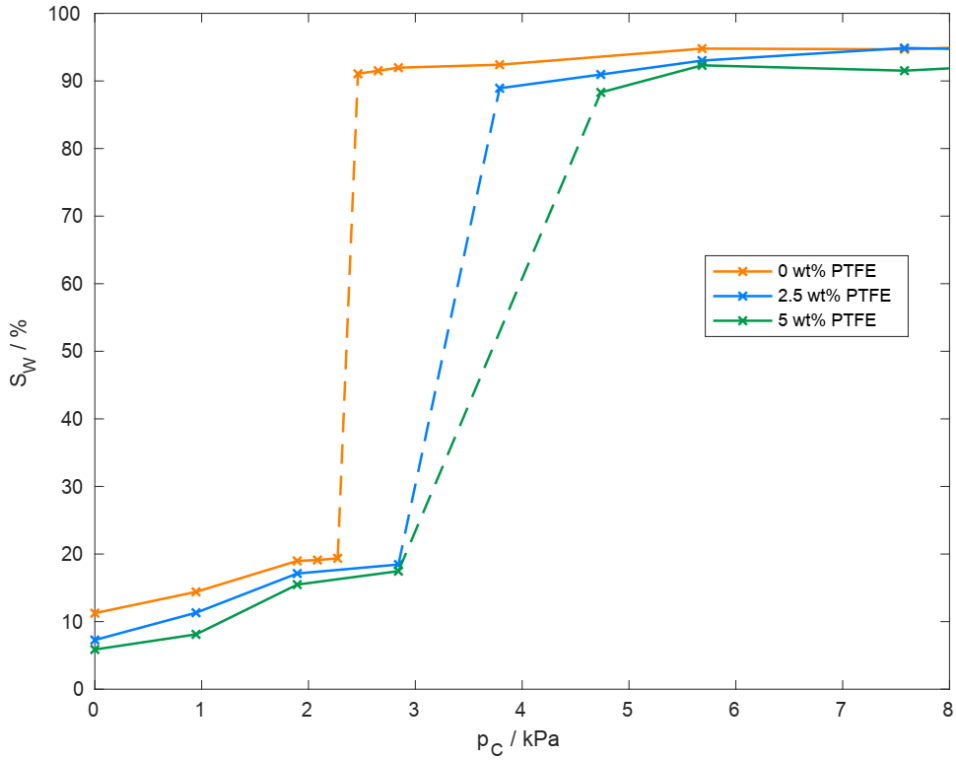

Figure 6: Simulated capillary pressure-saturation curves for hydrophobic binder contents of 0, 2.5 and 5 wt%.

Acknowledgement

The research leading to these results has received funding from the European Union's Horizon 2020 research and innovation program within the project ID-Fast: Investigations on degradation mechanisms and Definition of protocols for PEM Fuel cells Accelerated Stress Testing, under grant agreement n°779565.

References

[1] L. Cindrella et al., Journal of Power Sources, 2009, 194(1):146-160
[2] D. H. Rothman, J. M. Keller, Immiscible cellular-automaton fluids, Journal of Statistical Physics 1988, 52:1119–1127
[3] J. Wang, H. Wang, Y. Fan, Techno-Economic Challenges of Fuel Cell Commercialization, Engineering 2018, 4:352-360
[4] S. G. Kandlikar, M. L. Garofalo, Z. Lu, Water Management in A PEMFC: Water Transport Mechanism and Material Degradation in Gas Diffusion Layers, Fuel Cells 2011, 11(6)
[5] T. Arlt et al., Influence of Artificial Aging of Gas Diffusion Layers on the Water Management of PEM Fuel Cells, ECS Electrochemistry Letters 2014, 3(2):F7-F9
[6] J. Wu, In situ accelerated degradation of gas diffusion layer in proton exchange membrane fuel cell Part I: Effect of elevated temperature and flow rate, Journal of Power Sources 2010, 195:1888-1894

[7] P. L. Bhatnagar, E. P.Gross, M. Krook, A Model for Collision Processes in Gases: I. Small Amplitude Processes in Charged and Neutral One-Component Systems, Physical Reviews 1954, 94:511–525
[8] M. C. Sukop, D. T. Thorne, Lattice Boltzmann Modeling: An Introduction for Geoscientists and Engineers, 2006, 1st ed., Springer Berlin Heidelberg
[9] T. Reis, T. N. Phillips, Lattice Boltzmann model for simulating immiscible two-phase flows, Journal of Physics A: Mathematical and Theoretical 2007, 40:4033–4053
[10] S. Leclaire, M. Reggio, J.-Y., Trépanier, Isotropic color gradient for simulating very high-density ratios with a two-phase flow lattice Boltzmann model, Computers & Fluids 2011, 48:98–112
[11] Liu, H.; Valocchi, A. J.; Kang, Q. Three-dimensional lattice Boltzmann model for immiscible two-phase flow simulations, Physical Review 2012, 85:046309
[12] J. Tölke et al., Lattice Boltzmann simulations of binary fluid flow through porous media, Philosophical transactions. Series A, Mathematical, physical, and engineering sciences 2002, 360:535–545
[13] B. Chopard, A. Dupuis, A. Masselot, and P. Luthi, Cellular automata and lattice Boltzmann techniques: an approach to model and simulate complex systems, Advances in Complex Systems 2002, 05(02):103-246
[14] Latva-Kokko, M.; Rothman, D. Static contact angle in lattice Boltzmann models of immiscible fluids. Physical Review E 2005, 72:046701
[15] Q. Zou, X. He, On pressure and velocity boundary conditions for the lattice Boltzmann BGK model, Physics of Fluids 1997, 9(6):1591-1598
[16] http://www.accudynetest.com/polymer_surface_data/ptfe.pdf, Diversified Enterprises, 2009
[17] Surface properties of PEMFC gas diffusion layers, Journal of The Electrochemical Society 2010, 157(2):B195-B206